Journal of Renewable Materials

Tech Science Press

DOI: 10.32604/jrm.2022.019576

ARTICLE

Influence of Beta-Cyclodextrin Functionalized Tin Phenylphosphonate on the Thermal Stability and Flame Retardancy of Epoxy Composites

Yongming Chen[1,2,#], Shuai Huang[1,#], Han Zhao[1], Ru Yang[2], Yining He[1], Tianyu Zhao[1], Yunlong Zhang[1], Qinghong Kong[1,*], Shasha Sun[3,*] and Junhao Zhang[3]

[1]School of the Environment and Safety Engineering, Jiangsu University, Zhenjiang, 212013, China

[2]Zhenjiang Electric Power Supply Company, State Grid Jiangsu Electric Power Co., Ltd., Zhenjiang, 212000, China

[3]School of Environmental and Chemical Engineering, Jiangsu University of Science and Technology, Zhenjiang, 212003, China

[*]Corresponding Authors: Qinghong Kong. Email: kongqh@ujs.edu.cn; Shasha Sun. Email: sunshasha@just.edu.cn

[#]They contributed equally to this work

Received: 08 October 2021 Accepted: 20 December 2021

ABSTRACT

To enhance the thermal stability and flame retardancy of epoxy resin (EP), beta-cyclodextrin (β-CD) is successfully introduced into the layered tin phenylphosphonate (SnPP), which is incorporated into EP matrix for preparing EP/β-CD@SnPP composites. The results indicate that the addition of β-CD@SnPP obviously improve the thermal stability and residual yield of EP composites at higher temperature. When the amount of β-CD@SnPP is only 4 wt%, EP/4β-CD@SnPP composites pass V-1 rating, and LOI value is up to 30.8%. Meanwhile, β-CD@SnPP effectively suppress the heat release and reduce the smoke production of EP/β-CD@SnPP composites in combustion, and the peak heat release rate (PHRR), total heat release (THR), smoke production rate (SPR) of EP/6β-CD@SnPP composites reduce by 28.4%, 33.0% and 44.8% by comparison with those of pure EP. The good flame retardancy and smoke suppression are ascribed to the synergistic effect of excellent carbon-forming capability and fire retardancy of β-CD@SnPP.

KEYWORDS

Epoxy resin; tin phenylphosphonate; beta-cyclodextrin; synergistic effect; flame retardancy; smoke suppression

1 Introduction

Epoxy resin is widely used in various fields due to its excellent moisturizing performance, good heat resistance, good mechanical properties, such as in building, coating, composites, and so on [1–6]. However, the applications are severely limited due to the flammability and dripping tendency. In order to improve the flame retardancy, flame retardants must be used to achieve flame retardant requirements. In past decades, halogen-free additives have been widely interested due to environmental protection [7–10].

Phosphorous compounds have motivated interest from researchers worldwide because of their high efficiency, less smoke and low toxicity, which can act as flame retardant in both condensed and gaseous phases [11–15]. Phenylphosphate, as a kind of layered metal phosphate, not only has the characteristics of layered compounds, but also has good chemical stability, high thermal stability, simple preparation process, low cost and other characteristics [16,17]. Phenylphosphate modified polymer has been widely

investigated with excellent flame retardancy [18,19]. For example, ultrathin nickel phenylphosphate (NiPP) was added into epoxy resin for preparing EP/NiPP nanocomposites, which reveals that the thermostability and flame retardancy of EP/NiPP nanocomposites were obviously improved, and the maximum residual of EP/6 w% NiPP nanocomposites was high to 24.1% at 700°C due to excellent catalytic carbonization and fire retardant ability [20]. However, high content of phenylphosphate can worsen the mechanical performances of EP composites, but EP composites with low content of phenylphosphate cannot meet flame retardant requirements [21–23].

β-cyclodextrin (β-CD) has biodegradable, biocompatible, environmentally friendly and non-toxic features. Meanwhile, its molecular skeleton is rich in carbon and contains a certain amount of the side chain hydroxyl groups. In the process of thermal decomposition, they can be polymerized carbonization, which hinders the progress of combustion. At the same time, the released CO_2, H_2O and other non-toxic, non-corrosive and non-flammable gases have the effect of preventing combustion. Moreover, the hydroxyl groups on the β-CD molecule make it good reactivity, which can be introduced into the interlayers of layered compounds by molecular design [24–26].

Based on the above discussion, β-Cyclodextrin can form a large amount of carbon and release incombustible gas during combustion or pyrolysis. Metal phenyl phosphate not only has lamellar barrier effect, but also the transition metal compound obtained by its pyrolysis has the effect of catalyzing carbon formation, and phosphoric acid has excellent flame retardancy in both the condensed and gas phases. Therefore, it is an effective strategy that cyclodextrin is introduced between metal phenyl phosphate layers to play a synergistic effect in flame retardancy and smoke suppression. In this work, the layered tin phenylphosphonate (SnPP) was successfully synthesized by the coordination of Sn^{4+} and phenyl phosphonic acid. Then, SnPP was modified with β-CD, which was incorporated into EP matrix for preparing EP/β-CD@SnPP composites. The thermal properties and combustion properties of EP/β-CD@SnPP composites were studied. The results show that EP/β-CD@SnPP composites exhibited excellent thermal stability, flame retardancy and smoke suppression.

2 Experimental Section

2.1 Materials

Tin chloride ($SnCl_4{\cdot}4H_2O$, ACS reagent, ≥98%), polyvinyl pyrrolidone (PVP, 360), ethylene glycol (ACS reagent, ≥99%), hexamethylenetetramine, (ACS reagent, ≥99%), and ethanol (ACS reagent, ≥99%) were supplied by Sigma Aldrich, Ltd. (Shanghai, China). 4, 4'-Diaminodiphenyl sulfone (>97%), beta-cyclodextrin ($C_{42}H_{70}O_{35}$, >97%) and phenylphosphonic acid ($C_6H_7O_3P$, >98%) were purchased from TCI Chemicals Company. Epoxy resin (NPEL128) was purchased from South Asia Electronic Materials Co., Ltd. (Kunshan, China).

2.2 Synthesis of Tin Phenylphosphonate

5.1 g phenylphosphonic acid was evenly dispersed in 100 cm^3 deionized water using ultrasound and stirring, forming solution A. 5.28 g $SnCl_4{\cdot}4H_2O$ was dissolved into another 100 cm^3 deionized water with stirring, forming solution B. Then, the above two solutions were mixed with stirring for 24 h at room temperature. The precipitation was collected by centrifugation and washed by deionized water, and dried in a vacuum oven at 60°C for 24 h. The obtained product is tin phenylphosphonate (Sn(IV) $(C_6H_5PO_3)_2$, SnPP).

2.3 Synthesis of β-CD@SnPP

Firstly, 1 g β-CD was dispersed into 50 cm^3 deionized water to form a dispersed liquid C. Then, the dispersed liquid C and solution B were slowly added to solution A in turn, which was stirred at room

temperature for 24 h. The precipitation was collected by centrifugation and washed by deionized water, and dried in a vacuum oven at 60°C for 24 h. The product was labeled as β-CD@SnPP.

2.4 Preparation of EP/β-CD@SnPP Composites

EP/β-CD@SnPP composites were prepared by solution blending method. The specific process was as follows: β-CD@SnPP was added in a moderate amount of acetone solution under ultrasonic dispersion for 30 min, and EP was added to the above dispersion under ultrasound for 30 min. Then it was stirred and heated at 90°C until acetone was completely volatilized. Afterwards, an appropriate amount of DDM (EP:DDM = 4:1) was added into the above mixture, which was stirred continuously until DDM was completely dissolved. After the resulting mixture was evacuated to remove bubbles, it was poured into the mold and cured at 100°C for 1 h. Finally, the sample was cured by temperature according to the curing process: 110°C for 2 h, 130°C for 2 h, 150°C for 2 h. The preparation process of EP/4SnPP was consistent. The specific formulations are presented in Table 1.

Table 1: Ingredients and TGA data of pure EP and EP composites

Samples	EP (wt%)	β-CD@SnPP (wt%)	$T_{5\%}$ (°C)	T_{max} (°C)	Residues (wt%, 700°C)
Pure EP	100	0	350.2	408.5	17.9
EP/2β-CD@SnPP	98	2	343.7	403.4	23.5
EP/4β-CD@SnPP	96	4	341.2	405.8	25.8
EP/6β-CD@SnPP	94	6	337.3	404.5	27.2
EP/4SnPP	96	4SnPP	334.1	405.6	25.3

2.5 Characterization

The morphologies of CD@SnPP and SnPP were investigated by scanning electron microscopy (SEM, Zeiss EVOMA15). The compositions and structures of β-CD@SnPP and SnPP were characterized by X-ray diffraction pattern (XRD, MAX-RB, Cu Ka radiation with the angle ranged from 5° to 70°) and Fourier transform infrared spectroscopy (FTIR, Nicolet 6700 spectrometer with the frequency range from 400 to 4000 cm^{-1}). The thermal stability of the samples was studied by a TA Q50 thermo-analyzer instrument with a heating rate of 10 °C/min in N_2 atmosphere. The limiting oxygen index (LOI) values specimens with sizes of 130 × 6.5 × 3.2 mm^3 were measured through a HC-2 oxygen index model instrument, and the UL-94 rating of specimens with size of 130 × 12.7 × 3.2 mm^3 through a burning chamber. The combustion data of EP/β-CD@SnPP and EP/SnPP composites were acquired from a cone calorimeter (FTT, UK), observing the stipulation in ISO 5660-1. Each specimen (100 × 100 × 4 mm^3) was irradiated at a heat flux of 35 kW/m^2.

3 Results and Discussion

3.1 The Structure of SnPP and β-CD@SnPP

SEM images of SnPP and β-CD@SnPP are provided in Fig. 1. The results show that SnPP and β-CD@SnPP have similar shape and size, indicating simple modification of β-CD does not change the shape and size, and the size is from 100 to 200 nm. However, these particles have a certain degree of agglomeration and stacking. X-ray diffraction method is always used to examine the structure of layered compound [27–29]. Fig. 2a shows XRD spectra of SnPP and β-CD@SnPP, and the diffraction peaks appeared at 2θ = 6.1° and 12.1° correspond to (010) and (020) diffraction planes of SnPP, which are characteristic peaks of layered structure [30]. Fig. 2b is the FTIR spectra of SnPP and β-CD@SnPP. The

small peak at 3051 cm^{-1} is assigned to C-H on the benzene ring. The peaks of 740, 692 and 1726 cm^{-1} are stretching vibration of C-P. The peaks at 1048 and 1138 cm^{-1} can be ascribed to the characteristic absorption peak of $–P(O)(OH)_2$. Compared with the FTIR spectrum of phenyl phosphonic acid, the characteristic vibration peaks of $–P(O)(OH)_2$ near 1000 cm^{-1} changes greatly, which is attributed to the bonding of Sn^{4+} and $C_6H_5PO_3^{2+}$ [31,32]. In addition, compared with the absorption peak of SnPP, the peak at 1439 cm^{-1} is the representative -OH vibration peak in the β-CD molecule. The above results indicate that β-CD@SnPP was successfully synthesized [33]. Figs. 2c and 2d are TGA and DTG curves of SnPP and β-CD@SnPP. As shown in the TGA curves, the thermal degradation of SnPP and β-CD@SnPP are divided into two stages. The first stage is occurred before 270°C. The mass loss is 6.6 wt% and 5.9 wt%, respectively, which is mainly attributed to the crystal water in the molecular structure of SnPP and β-CD@SnPP, the adsorbed water on the surface and some volatile components [34]. Subsequently, the obvious weight losses between 270°C and 640°C in the second stage are 25.3 wt% and 24.7 wt%, respectively, which can be explained that SnPP is decomposed to Sn compounds, phosphorous compounds and organic small molecules, and beta-cyclodextrin is pyrolyzed into carbon.

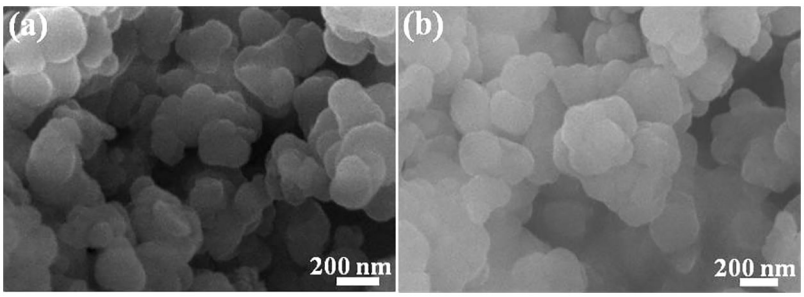

Figure 1: (a) SEM image of SnPP; (b) SEM image of β-CD@SnPP

3.2 The Thermal Stability of EP/β-CD@SnPP Composites

To study the influence of β-CD@SnPP on the thermal stability of EP composites, Fig. 3 and Table 1 exhibit the TGA curves, thermal analysis data and residue yields. From the results, pure EP pyrolyzes rapidly between 345°C and 468°C, which is essentially the same as the pyrolysis temperature range of β-CD@SnPP. The $T_{5\%}$ (the onset decomposition temperature) and T_{max} (the maximum decomposition temperature) of pure EP are 350.2°C and 408.5°C, and the residual amount is approximately 17.9% at 700°C. For comparison, the $T_{5\%}$ values of EP composites with 2 wt%, 4 wt% and 6 wt% β-CD@SnPP are reduced to 343.7°C, 341.2°C and 337.3°C, and the T_{max} values are also reduced to 403.4°C, 405.8°C and 404.5°C. However, the thermostability of EP/β-CD@SnPP composites is significantly enhanced above 400°C, which illuminate that β-CD@SnPP has a low initial pyrolysis temperature, and the addition of β-CD@SnPP can improve the thermal stability of EP composites at higher temperature. At 700°C, the residues of EP/β-CD@SnPP composites are increased evidently. Increasing the amount of β-CD@SnPP to 6 wt%, the residual amount of EP/6β-CD@SnPP composites reaches 27.2%. The improved thermostability and residual amount are mainly attributed to the appropriate thermal stability and excellent forming-carbon capacity of β-CD@SnPP [35]. According to the curves, the $T_{5\%}$ and T_{max} of EP/4SnPP composites are reduced to 334.1°C and 405.6°C, and the residue is 25.3% at 700°C. The results show that β-CD@SnPP has better carbon-forming ability than SnPP.

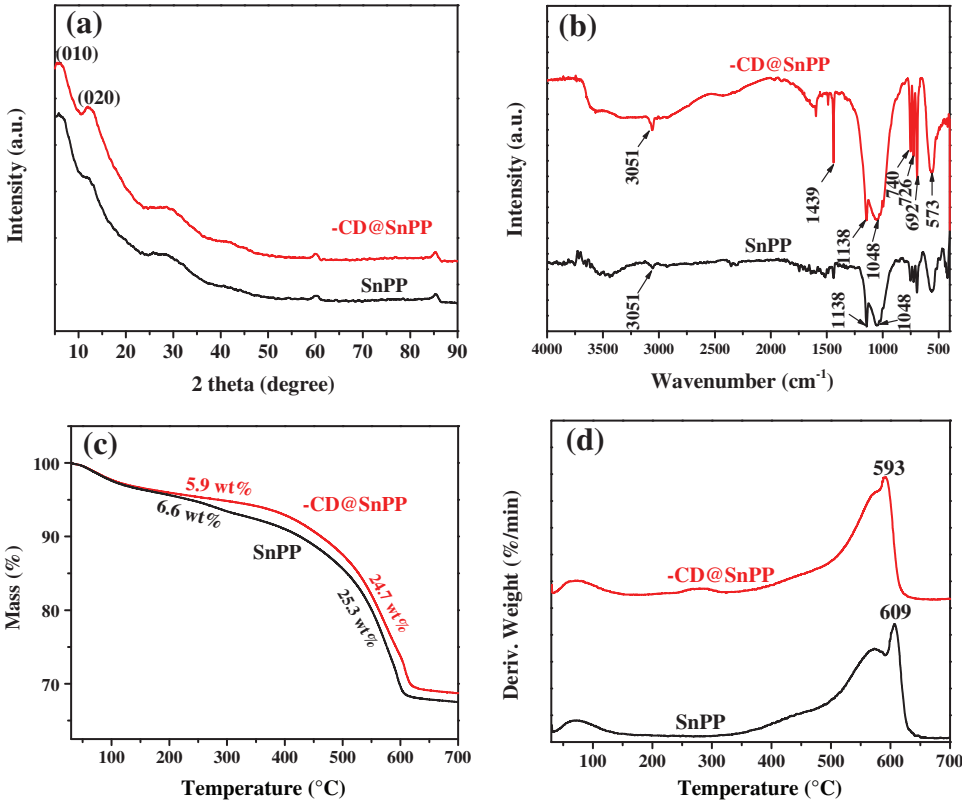

Figure 2: (a) XRD spectra of SnPP and β-CD@SnPP; (b) FTIR spectra of SnPP and β-CD@SnPP; (c) TGA curves of SnPP and β-CD@SnPP; (d) DTG curves of SnPP and β-CD@SnPP

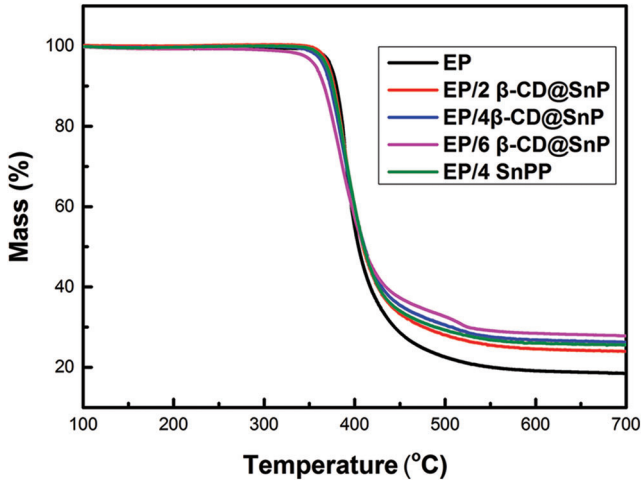

Figure 3: TGA curves of pure EP and EP composites in N_2

3.3 The Combustion Performance of EP/β-CD@SnPP Composites

To investigate the effect of β-CD@SnPP or synergistic effect of β-CD and SnPP on the flame retardancy in epoxy resin, the LOI and vertical burning tests were carried out with the results listed in Table 2. The results show that pure EP is combustible with an LOI value 25.9%, and there is no rating in UL-94 test.

Incorporating β-CD@SnPP, the LOI values and UL-94 ratings of EP/β-CD@SnPP composites are improved obviously. When 2 wt% β-CD@SnPP is incorporated into EP, the LOI value of EP/2β-CD@SnPP composites is risen to 28.5%, and it is still failed to pass the UL-94 test. With further increasing the amount of β-CD@SnPP, the LOI of EP/4β-CD@SnPP composites is 30.8% and it has passed UL-94 V-1 rating. However, the LOI value of EP/4SnPP composites is only 29.1%. The results indicate that β-CD and SnPP have excellent synergistic effect on flame retardancy, which is consistent with the results of thermal analysis. When the loading of β-CD@SnPP increases to 6 wt%, the LOI value drops back to 30.0% and it has passed UL-94 V-1 rating. The improved flame retardancy is mainly attributed to that nano-barrier effect of β-CD@SnPP, excellent synergistic flame-retardant capability of phosphorus containing species, Sn compound and β-CD [36,37].

Table 2: Parameters of pure EP and EP composites from LOI and UL-94 test

Samples	LOI%	UL-94
Pure EP	25.9	No rating
EP/2β-CD@SnPP	28.5	NR
EP/4β-CD@SnPP	30.8	V-1
EP/6β-CD@SnPP	30.0	V-1
EP/4SnPP	29.1	No rating

The effect of β-CD@SnPP on the burning behaviors of EP composites was evaluated through cone calorimeter, revealing some important parameters to comprehend the flame retardant and smoke suppression capabilities during burning progress [38]. Time to ignition (TTI) is a main indicator for determining flammability. The results show that the TTI of pure EP is 68 s, and it burnt quickly after being ignited with a large amount of smoke. When β-CD@SnPP and SnPP are incorporated into EP for preparing EP composites, the TTI values are increased obviously, which are attributed to that β-CD@SnPP has the barrier effect and thermal decomposition of β-CD releases non-flammable gas and forms carbon layer [39,40]. Fig. 4a provides the heat release rate (HRR) curves of EP/β-CD@SnPP composites, which distinctly exhibits neat EP burns violently once ignited, showing a sharp peak HRR (PHRR) with a value of 1189 $kW \cdot m^{-2}$. The PHRR values of EP/β-CD@SnPP composites exhibited a gradual decrease trend as raising the amount of β-CD@SnPP, and they are decreased to 1039, 954, 852 $kW \cdot m^{-2}$ when 2, 4 and 6 wt% β-CD@SnPP are added. Fig. 4b is the total heat rate (THR) curves of pure EP and EP composites. When the flame extinguishes, the THR value of neat EP is 88 MJ/m^2 at 400 s, and the values of EP composites with 2, 4 and 6 wt% β-CD@SnPP, are reduced to 77, 63, 59 MJ/m^2, respectively. However, 4 wt% SnPP is incorporated into EP matrix, the PHRR and THR values of EP/4SnPP composites still maintain 1015 $kW \cdot m^{-2}$ at 120 s and 74 MJ/m^2 at 400 s. The above results illuminate that β-CD@SnPP has better inhibition on heat release in contrast to SnPP, which is primarily ascribed to the synergistic effect of β-CD and SnPP that β-CD@SnPP can play a physical barrier, SnPP has a good catalytic carbonization effect for promoting the formation of carbon layer, and β-CD is dehydrated to form carbon layer during combustion [40,41]. As everyone knows, thick and dense carbonaceous barrier layer serves a vital role for heat and mass transfer, reducing heat release during burning progress [41].

In fire disasters, smoke and toxic gases cause the greatest damage to life, followed by flame and heat. More than 70% of misfortune or death are caused by smoke and toxic gases in fire accident [42]. Consequently, it is indispensable to investigate the release of smoke gas. Fig. 4c is the smoke production rate (SPR) curves for pure EP and EP composites, and incorporating β-CD@SnPP and SnPP remarkably

decreases the SPR. The peak SPR value of pure EP is 0.3384 m^2 s^{-1} at 100 s, while those of EP composites with 2, 4 and 6 wt% β-CD@SnPP are reduced to 0.2511 m^2 s^{-1} at 115 s, 0.2063 m^2 s^{-1} at 130 s and 0.1869 m^2 s^{-1} at 125 s, reducing 25.8%, 39.0% and 44.8%, respectively. Consistent with the heat release results, the peak smoke release rate of EP/4SnPP composite is also higher than that of EP/4β-CD@SnPP composites. The superior smoke inhibition of EP/β-CD@SnPP composites is ascribed to the dense carbonaceous protective layer containing tin oxide and phosphorous compounds, which can isolate EP composite from flame, oxygen and heat, and prevent small organic molecules obtained from pyrolysis of epoxy resin to diffuse into air [43]. Fig. 4d shows the mass loss curve of neat EP and EP composites, and the results display that the mass loss of neat EP is the largest, and the residual amount at 400 s is merely 32.4 wt%. When 2, 4 and 6 wt% β-CD@SnPP are added, the residual amound of EP composites are increased to 36.7%, 37.1% and 39.6%, respectively, which is due to excellent carbonization capability of β-CD@SnPP [44].

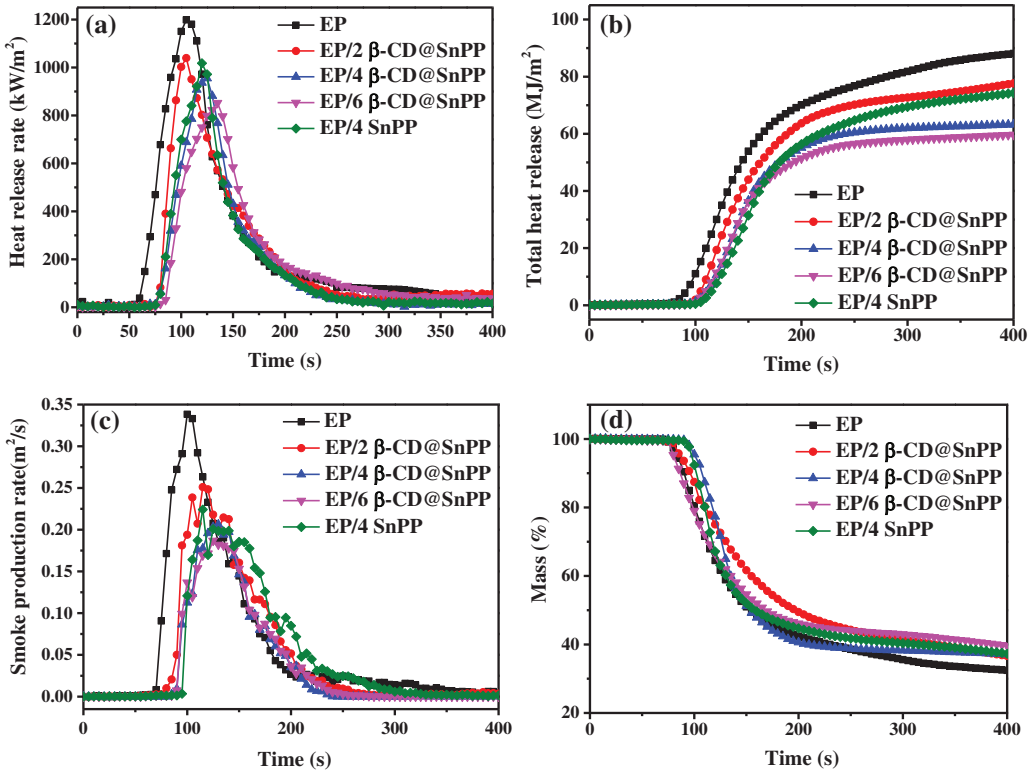

Figure 4: The results of pure EP and EP composites from CCTs at a heat flux of 35 kW/m^2: (a) HRR curves; (b) THR curves; (c) SPR curves; (d) Mass curves

Based on cone calorimetry tests, the results reveal that EP/β-CD@SnPP composites has good flame retardant and smoke suppression performances, which is mainly due to producing carbonaceous inorganic ceramic protective layer during the combustion process of EP/β-CD@SnPP composites [45,46]. To understand the effect of β-CD@SnPP on the carbonaceous ceramic isolation layer, Fig. 5 provides the SEM images of neat EP, EP/4SnPP, EP/4β-CD@SnPP and EP/6β-CD@SnPP composites after CCTs. The outer surface of the residual layer for pure EP is loose carbonaceous flimsy layer, as shown in Figs. 5a and 5b, and the internal residual layer interior is flimsy and crisp in Fig. 5c, which is mainly because pure epoxy resin quickly decomposes and burns, only producing a small amount of carbon. By

comparison of pure EP, the SEM images in Figs. 5d–5f illustrate that the residual amount of EP/4SnPP composites enhances, and the fluffy carbon layer on the outer surface of the external char layer becomes dense, while the inner surface forms dense carbon layer, but there are still some holes. Meanwhile, the internal hard carbon layer becomes thicker, but there are cracks. SnPP modified β-CD has better char-forming properties. When 4 wt% β-CD@SnPP is added, the outermost surface of the bulky carbon layer becomes less. Compared with EP/4SnPP composites, the hard carbon layer on the inner surface of the outer carbon layer becomes thicker, and the internal hard carbon layer becomes thicker and stronger, and there are fewer cracks. With further increasing the addition of CD@SnPP, the residual layer of EP/6β-CD@SnPP composites continues to strengthen and stabilize. Based on the above results, the thick and solid carbon layer can isolate the transfer of heat and oxygen between the gas phase and the condensed phase, inhibit combustion and improve flame retardancy and smoke suppression of EP/β-CD@SnPP composites [47].

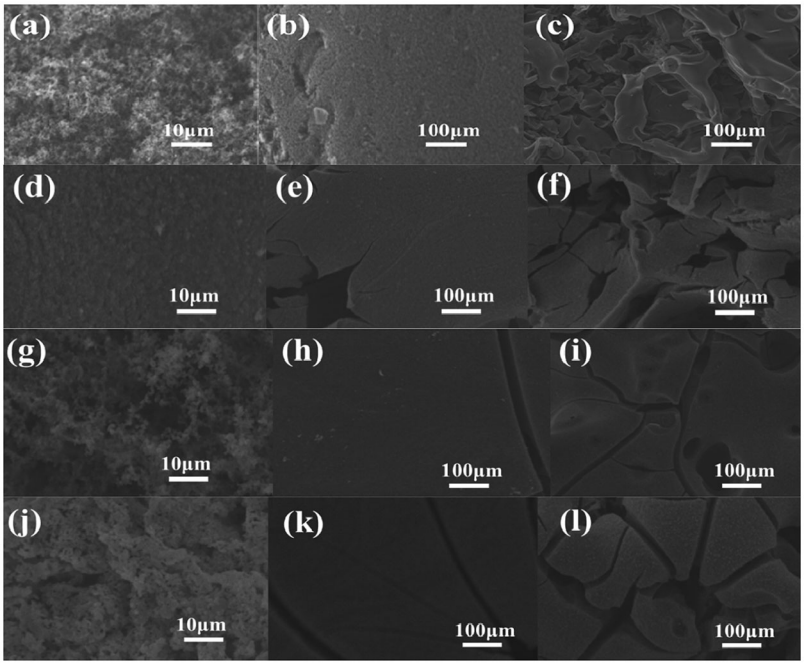

Figure 5: SEM images of outer char surface of (a, b) pure EP, (d, e) EP/4SnPP, (g, h) EP/4β-CD@SnPP, (j, k) EP/6β-CD@SnPP; SEM images of inner char surface of (c) pure EP, (f) EP/4SnPP, (i) EP/4β-CD@SnPP (l) EP/6β-CD@SnPP

4 Conclusions

In summary, β-CD@SnPP had been devised and synthesized, which was incorporated into EP matrix for preparing EP/β-CD@SnPP composites. The results of TGA revealed that β-CD@SnPP had suitable thermostability for EP, and β-CD@SnPP had excellent carbon-forming capability. The incorporation of β-CD@SnPP greatly improved the thermal stability of EP nanocomposites at higher temperature and residual yields of EP/β-CD@SnPP composites. The combustion results indicate that EP/4β-CD@SnPP composites passed UL-94 V-1 rating, and the LOI value was up to 30.8%. Moreover, the cone results evidenced that the addition of β-CD@SnPP obviously decreased the HRR, THR and SPR values, and improved the residues after the test. The PHRR, THR and SPR values of EP/6β-CD@SnPP composites were observably decreased by 28.4%, 33.0% and 44.8% compared with neat EP. The improved fire

retardation and smoke inhibition are ascribed to β-CD@SnPP with suitable thermal decomposition temperature, good forming carbon capacity and excellent synergistic flame-retardant effect, which is mainly due to the formation of dense and hard carbon-based inorganic ceramic layer, effectively isolate the transfer of heat and combustible gas between the EP/β-CD@SnPP composites composites and the combustion zone.

Funding Statement: This work was supported by Natural Science of Foundation of China (No. 21807050), Natural Science Foundation of Jiangsu Province (BK20180975), and Key Research and Development Program (Social Development) of Zhenjiang City (SH2019009), and Jiangsu University Student Innovation Training Project (2021102991025X).

Conflicts of Interest: The authors declare that they have no conflicts of interest to report regarding the present study.

References

1. Wang, X., Niu, H. X., Guo, W. W., Song, L., Hu, Y. (2021). Cardanol as a versatile platform for fabrication of bio-based flame retardant epoxy thermosets as DGEBA substitutes. *Chemical Engineering Journal, 421,* 129738. DOI 10.1016/j.cej.2021.129738.
2. Tang, L. C., Wan, Y. J., Yan, D., Pei, Y. B., Zhao, L. et al. (2013). The effect of graphene dispersion on the mechanical properties of graphene/epoxy composites. *Carbon, 60,* 16–27. DOI 10.1016/j.carbon.2013.03.050.
3. Nabipour, H., Qiu, S. L., Wang, X., Song, L., Hu, Y. (2021). Phosphorous-free ellagic acid-derived epoxy thermosets with intrinsic antiflammability and high glass transition temperature. *ACS Sustainable Chemistry & Engineering, 9(32),* 10799–10808. DOI 10.1021/acssuschemeng.1c02434.
4. Ye, G. F., Hou, S. Q., Wang, C., Shi, Q., Yu, L. F. et al. (2021). A novel hyperbranched phosphorus-boron polymer for transparent, flame-retardant, smoke-suppressive, robust yet tough epoxy resins. *Composites Part B-Engineering, 227,* 109395. DOI 10.1016/j.compositesb.2021.109395.
5. Mao, M., Yu, K. X., Cao, C. F., Gong, L. X., Zhang, G. D. et al. (2022). Facile and green fabrication of flame-retardant $Ti_3C_2T_x$ MXene networks for ultrafast, reusable and weather-resistant fire warning. *Chemical Engineering Journal, 427,* 131615. DOI 10.1016/j.cej.2021.131615.
6. Wan, Y. J., Tang, C. L., Yan, D., Zhao, L., Li, Y. B. et al. (2013). Improved dispersion and interface in the graphene/epoxy composite via a facile surfactant-assisted process. *Composite Science and Technology, 82,* 60–68. DOI 10.1016/j.compscitech.2013.04.009.
7. Yan, W., Xie, P., Yang, Z. W., Luo, G. J. (2020). Flame-retardant behaviors of aluminum phosphates coated sepiolite in epoxy resin. *Journal of Fire Sciences, 39,* 3–18. DOI 10.1177/0734904120934085.
8. Wang, X., Hu, Y., Song, L., Xing, W. Y., Lu, H. D. et al. (2010). Flame retardancy and thermal degradation mechanism of epoxy resin composites based on a DOPO substituted organophosphorus oligomer. *Polymer, 51(11),* 2435–2445. DOI 10.1016/j.polymer.2010.03.053.
9. Niu, H. X., Nabipour, H., Wang, X., Song, L., Hu, Y. (2021). Retardant epoxy thermoset with extremely low heat release rate and smoke emission. *ACS Sustainable Chemistry & Engineering, 9(15),* 5268–5277. DOI 10.1021/acssuschemeng.0c08302.
10. Liu, C., Wu, W., Shi, Y. Q., Yang, F. Q., Liu, M. H. et al. (2020). Creating MXene/reduced graphene oxide hybrid towards highly fire safe thermoplastic polyurethane nanocomposites. *Composites Part B: Engineering, 203,* 108486. DOI 10.1016/j.compositesb.2020.108486.
11. Yang, S., Wang, J., Huo, S. Q., Cheng, L. F., Wang, M. (2015). Preparation and flame retardancy of an intumescent flame-retardant epoxy resin system constructed by multiple flame-retardant compositions containing phosphorus and nitrogen heterocycle. *Polymer Degradation Stability, 119,* 251–259. DOI 10.1016/j.polymdegradstab.2015.05.019.
12. Nie, S. B., Liu, L., Dai, G. L., Zhou, C. (2017). Investigation on pyrolysis of intumescent flame-retardant polypropylene (PP) composites based on synchrotron vacuum ultraviolet photoionization combined with molecular-beam mass spectrometry. *Journal of Thermal Analysisand Calorimetry, 130,* 1003–1009. DOI 10.1007/s10973-017-6422-1.

13. Qiu, S. L., Ma, C., Wang, X., Zhou, X., Feng, X. M. et al. (2018). Melamine-containing polyphosphazene wrapped ammonium polyphosphate: A novel multifunctional organic inorganic hybrid flame retardant. *Journal of Hazard Materials, 344,* 839–848. DOI 10.1016/j.jhazmat.2017.11.018.
14. Vasiljevic, J., Jerman, I., Jaksa, G., Alongi, J., Malucelli, G. et al. (2015). Functionalization of cellulose fibres with DOPO-polysilsesquioxane flame retardant nanocoating. *Cellulose, 22,* 1893–1910. DOI 10.1007/s10570-015-0599-x.
15. Guo, W. W., Wang, X., Huang, J. L., Mu, X. W., Cai, W. et al. (2021). Phosphorylated cardanol-formaldehyde oligomers as flame retardant and toughening agents for epoxy thermosets. *Chemical Engineering Journal, 423,* 130192. DOI 10.1016/j.cej.2021.130192.
16. Zhou, T., Wu, T., Xiang, H. N., Li, Z. C., Xu, Z. L. et al. (2019). Simultaneously improving flame retardancy and dynamic mechanical properties of epoxy resin nanocomposites through synergistic effect of zirconium phenylphosphate and POSS. *Journal of Thermal Analysis and Calorimetry, 135,* 2117–2124. DOI 10.1007/s10973-018-7387-4.
17. Chen, K. X., Yang, D., Shi, Y. Q., Feng, Y. Z., Fu, L. B. et al. (2021). Synergistic function of N-P-Cu containing supermolecular assembly networks in intumescent flame retardant thermoplastic polyurethane. *Polymers for Advanced Technologies, 32(11),* 4450–4463. DOI 10.1002/pat.5448.
18. Cai, H. Y., Peng, F. C., Wang, Y. X., Yi, J. Y. (2020). Improving flame retardancy of epoxy resin nanocomposites by carbon nanotubes grafted CuAI-layered double hydroxide hybrid. *Journal of Nanoscience and Nanotechnology, 20(10),* 6406–6412. DOI 10.1166/jnn.2020.18120.
19. Xue, Y. C., Guo, X. M., Wu, M. R., Chen, J. L., Duan, M. T. et al. (2021). Zephyranthes-like Co_2NiSe_4 arrays grown on 3D porous carbon frame-work as electrodes for advanced supercapacitors and sodium-ion batteries. *Nano Research, 14,* 3598–3607. DOI 10.1007/s12274-021-3640-4.
20. Kong, Q. H., Zhu, H. J., Fan, J. S., Zheng, G. L., Zhang, J. H. et al. (2020). Boosting flame retardancy of epoxy resin composites through incorporating ultrathin nickel phenylphosphate nanosheets. *Journal of Applied Polymer Science, 138(16),* 50265. DOI 10.1002/app.50265.
21. Cai, Y. Z., Guo, Z. H., Fang, Z. P., Cao, Z. H. (2013). Effects of layered lanthanum phenylphosphonate on flame retardancy of glass-fiber reinforced poly(ethylene terephthalate) nanocomposites. *Applied Clay Science, 77–78(1),* 10–17. DOI 10.1016/j.clay.2013.03.015.
22. Tang, G., Liu, X. L., Yang, Y. D., Chen, D. P., Zhang, H. et al. (2020). Phosphorus-containing silane modified steel slag waste to reduce fire hazards of rigid polyurethane foams. *Advanced Powder Technology, 31(4),* 1420–1430. DOI 10.1016/j.apt.2020.01.019.
23. Tang, G., Liu, X., Zhou, L., Zhang, P., Deng, D. et al. (2020). Steel slag waste combined with melamine pyrophosphate as a flame retardant for rigid polyurethane foams. *Advanced Powder Technology, 31(1),* 279–286. DOI 10.1016/j.apt.2019.10.020.
24. Cong, Q., Ren, M., Zhang, T. T., Cheng, F. Y. (2021). Graphene/beta-cyclodextrin membrane: Synthesis and photoelectrocatalytic degradation of brominated flame retardants. *Chemstry Select, 6(32),* 8435–8445. DOI 10.1002/slct.202102235.
25. Zhang, J., Li, Z., Yin, G. Z., Wang, D. Y. (2021). Construction of a novel three-in-one biomass based intumescent fire retardant through phosphorus functionalized metal-organic framework and beta-cyclodextrin hybrids in achieving fire safe epoxy. *Composites Connunications, 23,* 100594. DOI 10.1016/j.coco.2020.100594.
26. Sag, J., Goedderz, D., Kukla, P., Greiner, L., Schönberger, F. et al. (2019). Phosphorus-containing flame retardants from biobased chemicals and their application in polyesters and epoxy resins. *Molecules, 24(20),* 3746. DOI 10.3390/molecules24203746.
27. Gao, M. Y., Tang, Z. H., Wu, M. R., Chen, J. L., Xue, Y. C. et al. (2021). Self-supporting N, P doped Si/CNTs/CNFs composites with fiber network for high-performance lithium-ion batteries. *Journal of Alloys and Compounds, 857,* 157554. DOI 10.1016/j.jallcom.2020.157554.
28. Guo, X. M., Zhang, W., Shi, J., Duan, M. T., Liu, S. J. et al. (2021). A channel-confined strategy for synthesizing CoN-CoOx/C as efficient oxygen reduction electrocatalyst for advanced zinc-air batteries. *Nano Research*. DOI 10.1007/s12274-021-3835-8.

29. Qian, C., Guo, X. M., Zhang, W., Yang, H. X., Qian, Y. et al. (2019). Co_3O_4 nanoparticles on porous bio-carbon substrate as catalyst for oxygen reduction reaction. *Microporous and Mesoporous Materials, 277,* 45–51. DOI 10.1016/j.micromeso.2018.10.020.
30. Kirumakki, S., Huang, J., Subbiah, A., Yao, J. Y., Rowland, A. et al. (2009). Tin(IV) phosphonates: Porous nanoparticles and pillared materials. *Journal of Materials Chemistry, 19(17),* 2593–2603. DOI 10.1039/b818618a.
31. Kong, Q. H., Sun, Y., Zhang, C., Guan, H., Zhang, J. H. et al. (2019). Ultrathin iron phenyl phosphonate nanosheets with appropriate thermalstability for improving fire safety in epoxy. *Composites Science and Technology, 182,* 107748. DOI 10.1016/j.compscitech.2019.107748.
32. Kirumakki, S., Samarajeewa, S., Harwell, R., Mukherjee, A., Herber, R. H. et al. (2008). Sn(IV) phosphonates as catalysts in solvent-free baeyer-villiger oxidations using H_2O_2. *Chemical Communications, 1(43),* 5556–5558. DOI 10.1039/b807938b.
33. Gomez-Alcantara, M. D., Cabeza, A., Olivera-Pastor, P., Fernandez-Moreno, F., Sobrados, I. et al. (2007). Layered microporous tin(IV) bisphosphonates. *Dalton Transactions, 2007(23),* 2394–2404. DOI 10.1039/b618762e.
34. Chen, J. L., Guo, X. M., Gao, M. Y., Wang, J., Sun, S. Q. et al. (2021). Free-supporting dual-confined porous Si@c-ZIF@carbon nanofibers for high-performance lithium-ion batteries. *Chemical Communications, 57(81),* 1580–10583. DOI 10.1039/D1CC04172J.
35. Shi, Y. Q., Liu, C., Duan, Z. P., Yu, B. (2020). Interface engineering of MXene towards super-tough and strong polymer nanocomposites with high ductility and excellent fire safety. *Chemical Engineering Journal, 399,* 125829. DOI 10.1016/j.cej.2020.125829.
36. Shan, X. Y., Han, J., Jiang, K. Y., Li, J. C., Xing, Z. X. (2019). Effect of $NiFe_2O_4$@graphene in intumescent flame-retarded poly(lactic acid) composites. *Polymer Composites, 40(2),* 652–656. DOI 10.1002/pc.24702.
37. Gao, C. Q., Shi, Y. Q., Chen, Y. J., Zhu, S. C. (2022). Constructing segregated polystyrene composites for excellent fire resistance and electromagnetic wave shielding. *Journal of Colloid and Interface Science, 606,* 1193–1204. DOI 10.1016/j.jcis.2021.08.091.
38. Gao, C. Q., Shi, Y. Q., Zhu, S. C., Fu, L. B. (2021). Induced assembly of polystyrene composites for simultaneously improving flame retardant and electromagnetic shielding properties. *Polymers for Advanced Technologies, 32(11),* 4251–4262. DOI 10.1002/pat.542.
39. Shi, Y. Q., Liu, C., Fu, L. B., Feng, Y. Z., Lv, Y. C. et al. (2021). Highly efficient MXene/nano-Cu smoke suppressant towards reducing fire hazards of thermoplastic polyurethane. *Composites Part A: Applied Science and Manufacturing, 150,* 106600. DOI 10.1016/j.compositesa.2021.106600.
40. Ding, J. M., Zhang, Y., Zhang, X., Kong, Q. H., Zhang, J. H. et al. (2020). Improving the flame-retardant efficiency of layered double hydroxide with disodium phenylphosphate for epoxy resin. *Journal of Thermal Analysis and Calorimetry, 140,* 149–156. DOI 10.1007/s10973-019-08372-9.
41. Li, D. F., Zhao, X., Jia, Y. W., He, L., Wang, X. L. et al. (2019). Simultaneously enhance both the flame retardancy and toughness of polylactic acid by the cooperation of intumescent flame retardant and bio-based unsaturated polyester. *Polymer Degradation and Stability, 168,* 108961. DOI 10.1016/j.polymdegradstab.2019.108961.
42. Nabipour, H., Wang, X., Song, L., Hu, Y. (2021). A high performance fully bio-based epoxy thermoset from a syringaldehyde-derived epoxy monomer cured by furan-derived amine. *Green Chemistry, 23(1),* 501–510. DOI 10.1039/D0GC03451G.
43. Kong, Q. H., Wu, T., Zhang, J. H., Wang, D. Y. (2018). Simultaneously improving flame retardancy and dynamic mechanicalproperties of epoxy resin nanocomposites through layered copper phenylphosphate. *Composites Science and Technology, 154,* 136–144. DOI 10.1016/j.compscitech.2017.10.013.
44. Li, Z., Zhang, J., Duffose, F., Wang, D. Y. (2018). Ultrafine nickel nanocatalyst-engineering of an organic layered double hydroxide towards a super-efficient fire-safe epoxy resin via interfacial catalysis. *Journal of Materials Chemitry A, 6(18),* 8488–8498. DOI 10.1039/c8ta00910d.
45. Yu, Z. R., Mao, M., Li, S. N., Xia, Q. Q., Cao, C. F. et al. (2021). Facile and green synthesis of mechanically flexible and flame-retardant clay/graphene oxide nanoribbon interconnected networks for fire safety and prevention. *Chemical Engineering Journal, 405,* 126620. DOI 10.1016/j.cej.2020.12662.

46. Guo, K. Y., Wu, Q., Mao, M., Chen, H., Zhang, G. D. et al. (2020). Water-based hybrid coatings toward mechanically flexible, super-hydrophobic and flame-retardant polyurethane foam nanocomposites with high-efficiency and reliable fire alarm response. *Composites Part B: Engineering, 193,* 108017. DOI 10.1016/j.compositesb.2020.108017.
47. Decsov, K., Takacs, V., Marosi, G., Bocz, K. (2021). Microfibrous cyclodextrin boosts flame retardancy of poly(lactic acid). *Polymer and Degradation and Stability, 191,* 109655. DOI 10.1016/j.polymdegradstab.2021.109655.